

Optimizing the Duct Shape and Location for Improving Performance of Darrieus Wind Turbine

Taher G. Abu-El-Yazied^A, Ahmad M. Ali^A, Ahmad. M. Makady^B, and Islam M. Hassan^{A*}

^ADesign and Production Engineering Department, Faculty of Engineering, Ain Shams University, Cairo, Egypt

^BCollege of Technological Studies, PAAET, Kuwait

Accepted 05 Jan 2015, Available online 01 Feb 2015, Vol.5, No.1 (Feb 2015)

Abstract

This article studies the possibility of increasing the power output of Darrieus wind turbine using an optimized duct using Genetic Algorithm (GA) or a straight duct. Computational fluid dynamics (CFD) studies were conducted to optimize the geometrical parameters of the duct in order to achieve maximum possible wind velocity increase, keeping into account the size and cost constraints of the device. In this study, the resulted duct shape decreases the variation in torque over a cycle by appropriately directing the flow upstream and downstream the turbine while increasing power coefficient. At the operating point obtained maximum power, which is at a tip-speed ratio of 3.29, use of optimized duct makes the torque ripple (TRF) decreased by 84% from un-ducted wind turbine and the maximum power coefficient (C_p) is increased by 123%. By choosing the position of the turbine in the duct appropriately, it is shown that the minimum torque ripple and maximum power coefficient were observed when the turbine center coincided with the throat of the duct. Both straight ducted wind turbine and optimized ducted wind turbine have close maximum power coefficient, but optimized duct makes the torque ripple (TRF) decreased by 80% from straight ducted wind turbine wind turbine.

Keywords: Darrieus wind turbine, Genetic Algorithm, Optimum Wind duct geometry, Computational fluid Dynamics

1. Introduction

It is a well-known that wind energy is very important as one of clean energy resources, and wind rotors are the most important of the wind energy. There are two different physical principles to extract power from wind. The first of them is the airfoil drag method, and the second is the airfoil lift principle. The Darrieus turbine is the most common VAWT invented in 1931 (Musgrove 1987, Berg, Klimas et al. 1990, German 1997, Price 2006, Mohamed 2011). On the basis of the second principle, a lot of investigations aim to improve the performance of vertical axis wind turbine like Darrieus and Savonius by increasing wind velocity. The differences between an horizontal and a vertical axis wind turbine are many, including their utilization: horizontal axis wind turbine is popular for large scale power generation, while the vertical axis wind turbine is utilized for small scale power generation (Paraschivoiu 2002, Li and Li 2010).

In this study, a new duct is developed, for a given turbine design, that reduces the variation in torque over a cycle by appropriately directing the flow upstream and downstream the turbine while increasing power conversion (Malipeddi and

Chatterjee 2012, Kishore, Coudron et al. 2013). A duct has been designed to accomplish this. Subsequently, the effect of:

- The position of the turbine in the duct,
- The external shape of the duct on the torque ripple and power conversion of the turbine is studied in an attempt to optimize the duct geometry.

2. CFD Numerical Solution

Aerodynamics numerical analysis carried out in this study is detailed in another study of the present work authors (Musgrove 1987). We will concentrate here on what is different than that done there in (Musgrove 1987), regarding the new configurations of the present ducted turbine and the duct geometry optimization as well. The optimization flow objective parameters are chosen as follows:

The speed ratio (λ) is defined as:

$$\lambda = \frac{R\omega}{V} \quad (1)$$

The power coefficient, C_p , defined as:

$$C_p = \frac{P_{\text{mech}}}{\frac{1}{2}\rho AV^3} \quad (2)$$

*Corresponding author: Islam M. Hassan

Torque ripple factor, *TRF*, is expressed as:

$$TRF = \frac{T_{pk-pk}}{\bar{T}} \tag{3}$$

Where: *R*, is rotor radius, ω is the rotational angular speed, *V*, is the wind free stream velocity, P_{mech} is the generated mechanical power, ρ , is the wind air density, *A*, is the rotor projected area, and, T_{pk-pk} is the peak-to-peak amplitude of the instantaneous torque, and \bar{T} is the torque averaged over a complete rotational cycle. Torque ripple factor, *TRF*, gives a dimensionless quantity representative of the variation in torque that can be universally compared across various turbines. When the torque produced is almost steady, the value of the ripple factor approaching 1.

3. Optimization plan of the present duct geometry

Genetic Algorithm (GA) is the most popular type of Evolutionary Algorithms (EA). One seeks the solution of a problem in the form of strings of numbers, by applying operators such as recombination and mutation (Sivanandam and Deepa 2008, Mosavi 2010, Taher G. Abu-El-Yazied 2014). A fully automatic optimization finally takes place, using modeFRONTIER commercial program (decision-maker for the configurations to investigate), the commercial tool Gambit for geometry and grid generation (including quality check) and the industrial CFD code ANSYS-Fluent to compute the flow field around the turbines. As a result of the CFD computation the objective function(s) is determined, and stored in a result file. The procedure is automated using journal scripts (to restart Gambit, Fluent) and a commercial program modeFRONTIER calling all codes in the right sequence as shown in Fig.1.

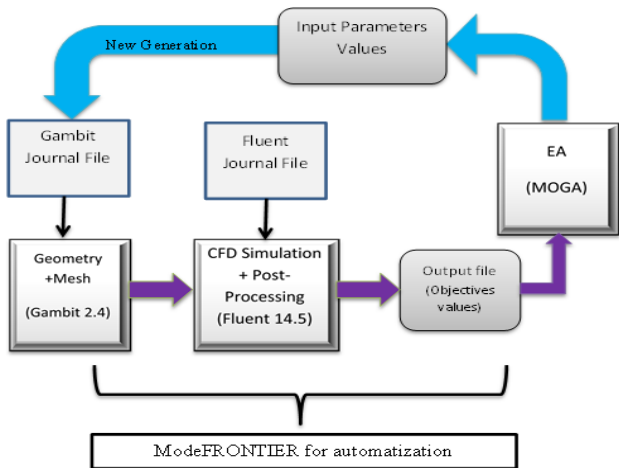


Fig.1 Schematic description of optimizer (MOGA) and CFD code coupling by modeFRONTIER

By checking the values stored in the result file, Multi Objective Genetic Algorithm (MOGA) is able to decide how to modify the input parameters before starting a

new generation. First generation of the input parameters is generated by using design of experiments based on a pseudo random called Sobol sequence; it works best with 2 to 20 variables. Both MOGA and Sobol are integrated algorithms inside modeFRONTIER program.

Simulations were carried out for both ducted and un-ducted turbine geometries. Details of the turbine chosen for simulation are given in Table 1. This turbine was adopted from the experimental work by M.R.Castalli (Castelli, Ardizzon et al. 2010, Taher G. Abu-El-Yazied May. 2014) . Thus, this turbine geometry will serve dual purpose of bringing out the importance of proper duct design besides being used as a test case of validation.

Table 1 Details of the turbine

D_{rotor} [mm]	1030
H_{rotor} [mm]	1414
n[-]	3
Blade profile	NACA 0021
A_s [m²]	1.236
C[mm] chord length	85.8
Solidity σ[-]	0.25

4. Description of the numerical flow field

Three separate zones are created, rotor zone being rotary, square far-field being stationary and shaft field being stationary as shown in Fig.2 .

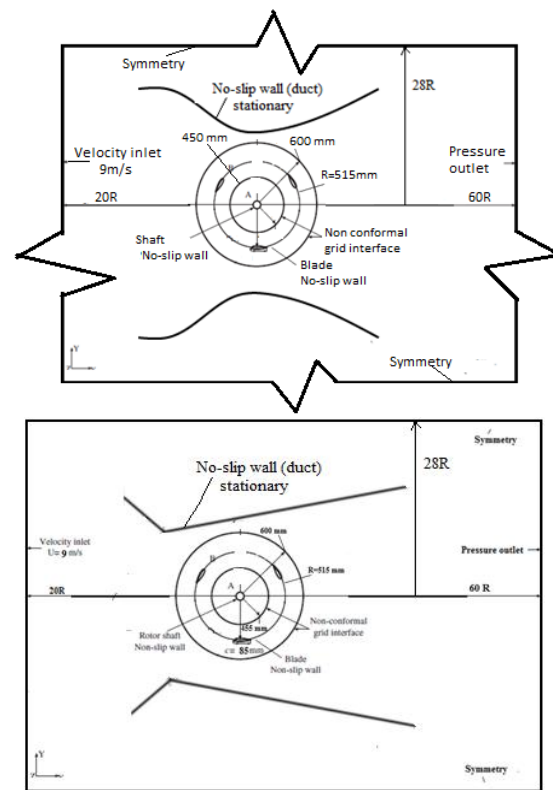


Fig.2 Schematic of the computational domain for curved and straight duct shape

The far-field mesh which is of hexahedral type is less dense as compared to hexahedral mesh in the rotary zone. Inlet was set as a velocity inlet, with a constant velocity profile of 9 m/s, while outlet was set as a pressure outlet.

Two symmetry boundary conditions were used for the two side walls. The appropriate size of the computational domain has been investigated. A computational domain of increasing dimensions (square domain of size, suitably normalized by the rotor radius R, in this work, the ratio between the square domain length and the rotor radius shown in Fig.2.

5. Main features of the numerical simulations

A complete campaign of simulations, based on full RANS unsteady calculations, was performed for a three bladed rotor architecture characterized by a NACA 0021 airfoil. The tip speed ratio (λ) was varied from a value of $\lambda=1.44$ (which corresponds to an angular velocity of $\omega=25.1$ rad/s) to $\lambda=3.8$ (which corresponds to an angular velocity of $\omega=66.41$ rad/s). These conditions made a blade Reynolds numbers equal $5.3 \cdot 10^4$.

The blade Reynolds number for this work was defined as:

$$Re = \frac{\rho V c}{\mu} \tag{4}$$

The dynamic viscosity (μ) was assumed to be $1.78 \cdot 10^{-5}$ Pa·s, the density (ρ) was set to 1.225 kg/m³ and the free stream velocity (V) was set to 9 m/s.

The effect of the turbulence model is verified and shown in Fig.3. These results give a good agreement obtained between published experiments(Castelli, Ardizzon et al. 2010) and Numerical CFD (Taher G. Abu-El-Yazied May. 2014) for the target function, C_p , when using the realizable k- ϵ turbulence model. Same tendency has been observed for other studies, proving the interest of this model for fast CFD simulations. This model is usually recommended for rotating bodies. The realizable k- ϵ model usually provides improved results for swirling flows and flow involving separation when compared to the standard k- ϵ model. The near-wall treatment relies on standard wall functions. The present study involves the application of SIMPLE scheme. Among several special discretization schemes available in FLUENT, Least squares cell based gradient with Standard pressure and second order upwind scheme are found to be appropriate for the present study. Simulation begins with continues with the second order, and among several Transient formulation available second order implicit are found to be appropriate for the present work. Convergence criterion for the solution is set as 10^{-5} . Currently, our area of consideration is to determine the forces acting on each of the three rotating airfoils and to obtain an optimum value of tip speed ratio which gives the

maximum power output when wind passes the turbine at a speed of 9 m/s.

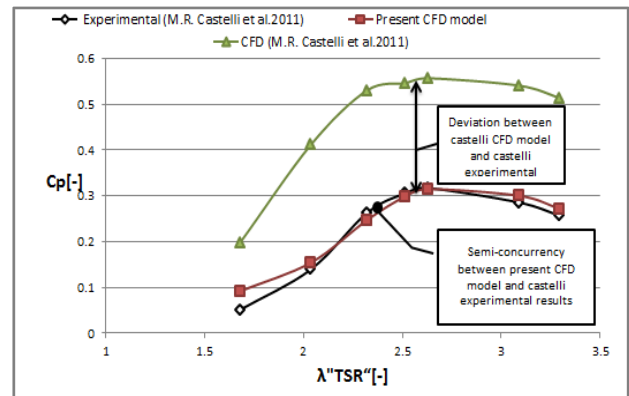


Fig.3 Verification of computational model, compared to published experimental and CFD results for a Darrieus turbine (Castelli, Ardizzon et al. 2010, Taher G. Abu-El-Yazied May. 2014)

Ten complete revolutions are often computed, using a calculated time-step for each tip speed ratio; the first revolutions is used to initiate the correct flow solution, while the flow properties (in particular the power coefficient C_p and the torque coefficient C_m) are obtained by averaging the results during the last two revolutions. 1500 iterations solved in steady flow first to initialize solution to unsteady flow. For optimization each case from each generation solved as a steady state problem and 500 iterations are solved in a steady state flow.

Ten complete revolutions are often computed, using a calculated time-step for each tip speed ratio; the first revolutions is used to initiate the correct flow solution, while the flow properties (in particular the power coefficient C_p and the torque coefficient C_m) are obtained by averaging the results during the last two revolutions. 1500 iterations solved in steady flow first to initialize solution to unsteady flow. For optimization each case from each generation solved as a steady state problem and 500 iterations are solved in a steady state flow.

6. Optimization methodology for curved duct shape

The following steps represent the optimization methodology of the present work:

A- Optimizing duct shape

- Identifying physical quantity required to be maximized; which is velocity inside duct.
- Creating gambit journal file after modeling duct without turbine using 7 points and identifying the Cartesian location of each point as a parameter as shown in Figure 4.
- Creating fluent journal file to solve a steady state solution for duct without turbine and its output will be the velocity inside duct at Specific position of duct throat w.r.t turbine.

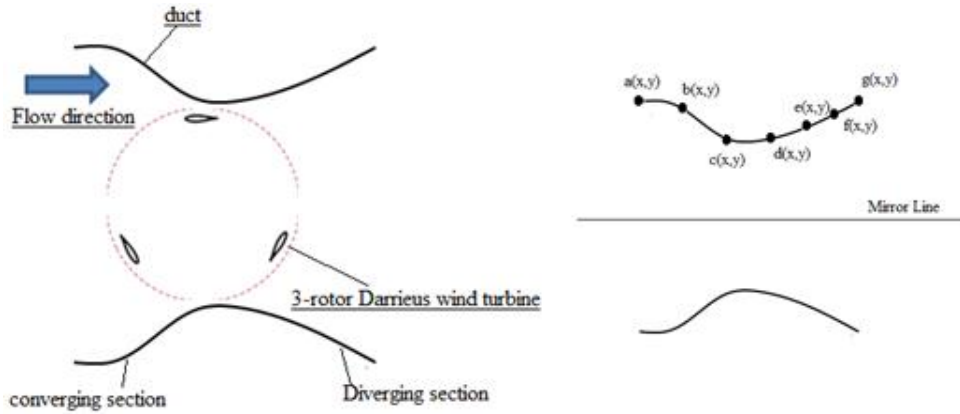


Fig.4 Schematic description of the free optimization parameters characterizing a duct shape, duct parameters (a_x ; a_y ; b_x ; b_y ; c_x ; c_y ; d_x ; d_y ; e_x ; e_y ; f_x ; f_y ; g_x and g_y)

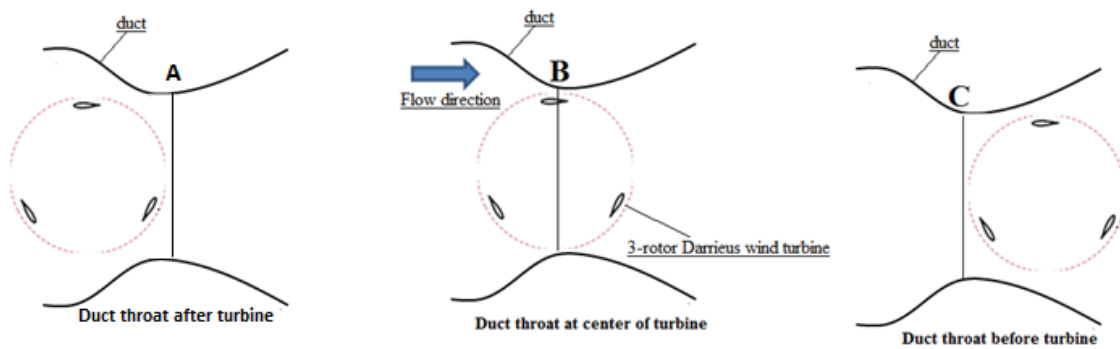


Fig.5 Variation of maximum velocity position to optimize duct shape according to it

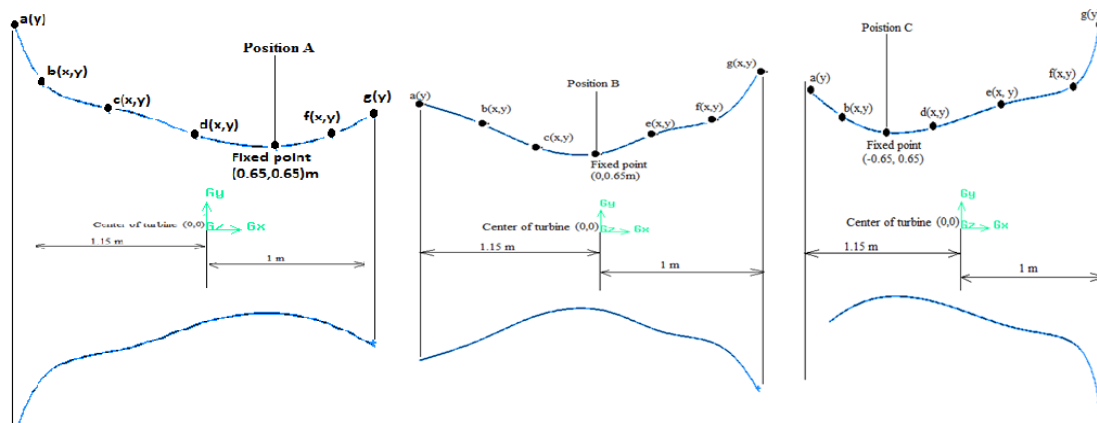


Fig.6 Schematic description of the free optimization parameters used to modify the duct shape at different positions optimal duct shapes from optimization

- Estimating the location of three positions to be investigated
- Performing optimization loop as mentioned in position A then repeat optimization at positions B and C as shown in Fig.5
- Obtaining optimal duct shapes at A, B and C as shown in Fig.6.

- Solving a transit problem for each optimal ducted turbine to estimate torque coefficient using fluent software
- Estimating power coefficients C_p at different tip speed ratios λ

7. Design parameters of straight duct shape

It was decided to simplify the diffuser geometry. As shown in Fig.7, the diffuser consisted of two parts: a converging section and a diverging section. There are essentially two geometrical parameters which needed to be optimized, namely (a) converging section half

B-Estimating values of power coefficient

- Designing mesh for each optimal shape including turbine using gambit software

cone angle and (b) diverging section half cone angle . Computational fluid dynamics (CFD) has been used in literature to model the duct design. The effect of each geometrical parameter on the Velocity augmentation was extensively examined and an optimal geometry was derived.

8. Discretization of the Numerical Flow Field

All created meshes as shown in Fig.8 with the same element grid size on blade 0.71 mm and growth factor 1.1 .Turbulence model used in this work is Realizable K-ε Turbulence model with standard wall function. After implementing simulation software we found that the y^+ values found in present work near all walls are around 40 which fall within the recommended range [Best-practice CFD ($30 < y^+ < 300$)].

9. Results and Discussion

The results reveal that it is possible to improve the performance of Darrieus turbine on multiple fronts using an appropriately optimized duct. An attempt was made at optimizing the shape of the duct by studying the effect of the position of the turbine and the external shape of the duct on the output of the Darrieus turbine. It was observed that these parameters have an optimum value. The main conclusions from this study are listed below:

A. Power Coefficient, C_p results for optimized duct shapes

In the same way, numerical analysis has been made for different optimized ducted turbines. The power performance C_p values obtained for each duct shapes at the values of different tip-speed ration λ as shown in Fig.9.

- Effect of turbine position inside duct on power coefficient. The best position will be at duct throat where power performance equal 0.69 at TSR 3.29 as shown in Fig 10.

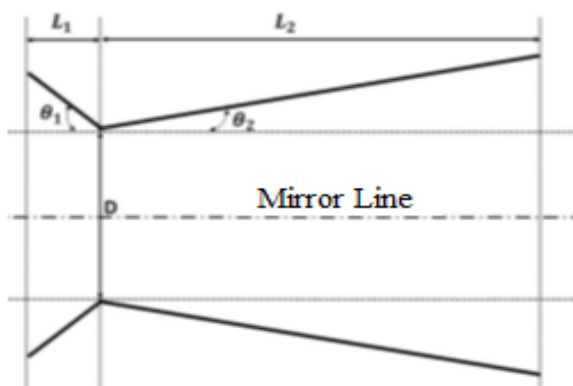


Fig.7 An initial 2d design of straight duct modeled using CFD

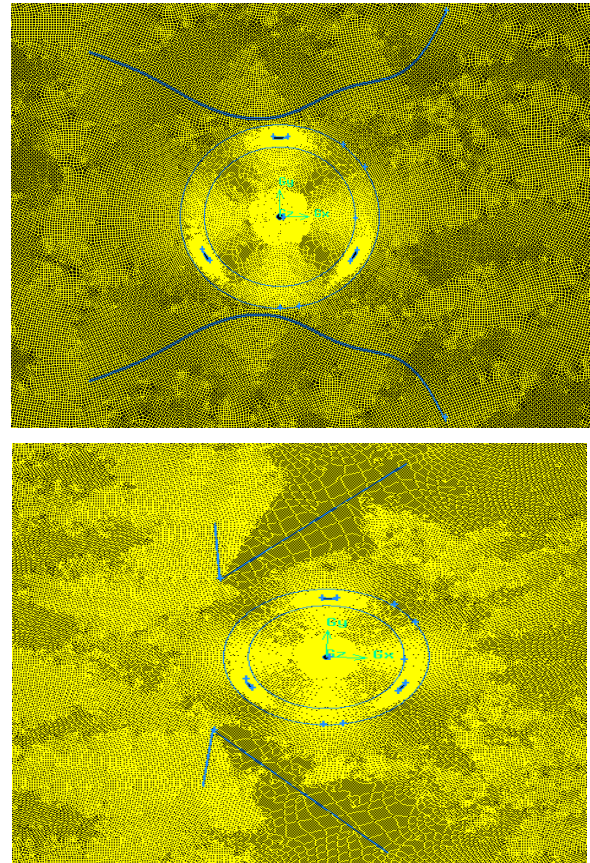


Fig.8 Mesh generated around curved duct and straight duct

B. Torque ripple, TRF results for optimized duct shapes

Fig.11 shows ripple factor respectively for these three optimal ducted turbine and ductless turbine. It is observed with respect to different tip-speed ratio. The lower values occurred at ducted turbine A and B.

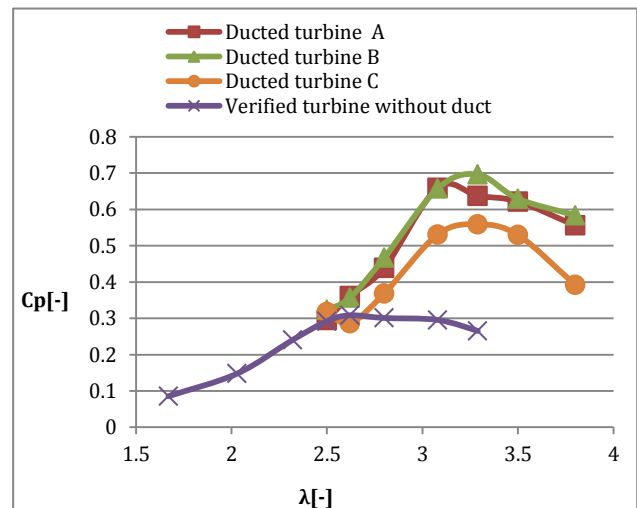


Fig.9 the power coefficient of the turbine with the duct as a function of the tip-speed ratio for $V =9m/s$

Fig. 12 display the distribution of the instantaneous power coefficient as a function of time for the rotor

blades and for optimum TSR for each model, showing that the contribution of each blade to overall rotor performance. Three peaks according to number of blades of the instantaneous power coefficient can be seen.

- Lowest torque ripple was found when the turbine center at the duct throat as in position B and equal 0.239 with λ equal 3.29 at maximum power coefficient as shown in Fig.13.

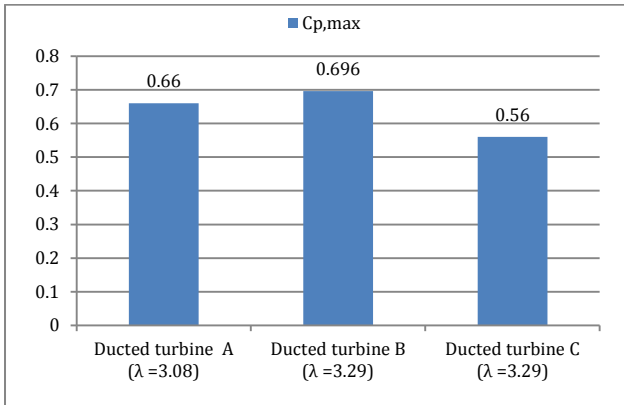


Fig.10 Effect of duct throat position on maximum power coefficient

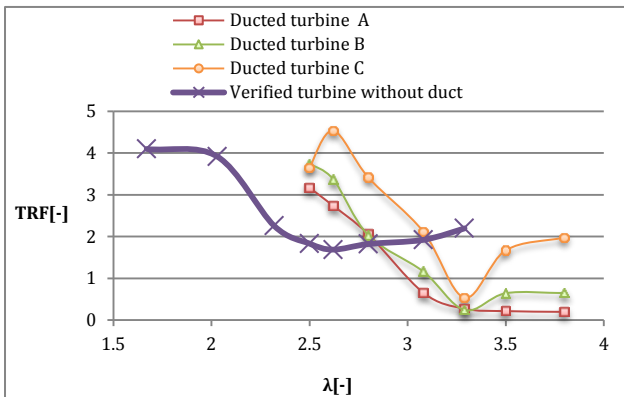


Fig.11 Comparison of torque ripple factor for optimal ducted turbines and ductless turbine, at various TSR

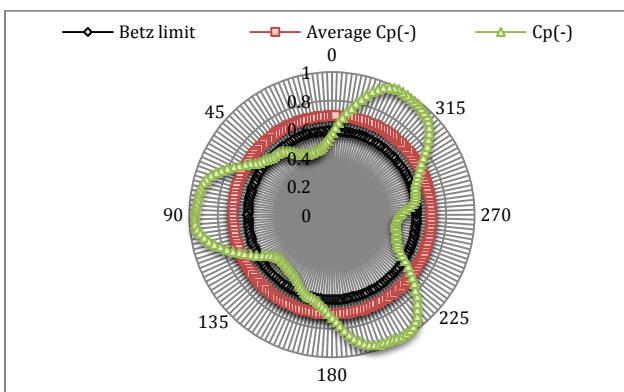


Fig.12 Value of instantaneous C_p as a function of azimuth angle θ for optimize ducted turbine B and the Betz's limit at $\lambda_{Cp,max}$ equal 3.29

C. Comparison between straight and optimized ducted turbine

In the same way, numerical analysis has been made for different barrier angles (θ_1 and θ_2) as shown in Fig. 14 and Fig. 15. This numerical analysis is made through straight duct with converging section length L_1 equal 50 cm and diverging section length L_2 equal to 125 cm, shows the angle-related changes of the power performance C_p values obtained for the straight duct through numerical analysis made at the values of different tip-speed ratio λ .

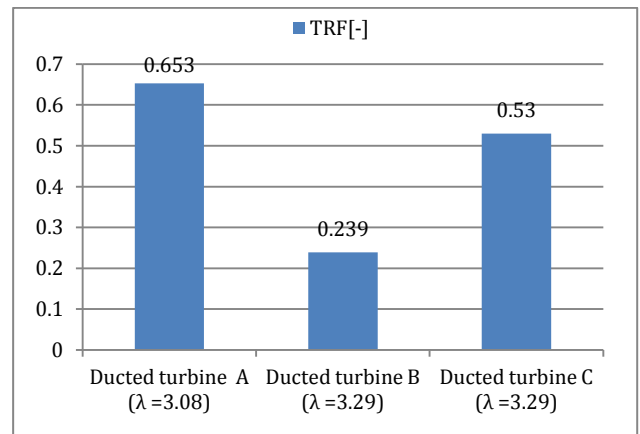


Fig.13 Effect of duct throat position on torque ripple factor at maximum power coefficient

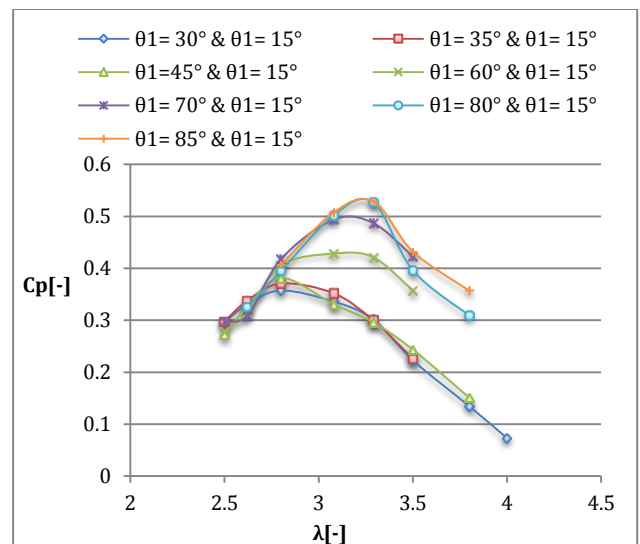


Fig.14 the power coefficient of the turbine with the straight duct as a function of the tip-speed ratio for $V=9m/s$ at $\theta_2=15^\circ$ and different values for θ_1

- External shape: The duct with straight external shape is observed to have close performance with a peak power coefficient of 0.67 $\theta_1=85^\circ$ and $\theta_2=45^\circ$ compared with optimized curved shape B. But optimized ducted turbine have lower torque ripple than straight ducted turbine as shown in Fig.16

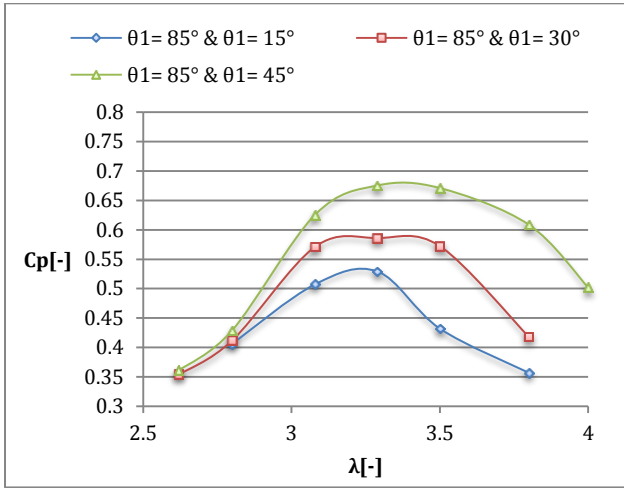


Fig.15 The power coefficient of the turbine with the straight duct as a function of the tip-speed ratio for $V=9\text{m/s}$ at $\theta_1=85^\circ$ and different values for θ_2

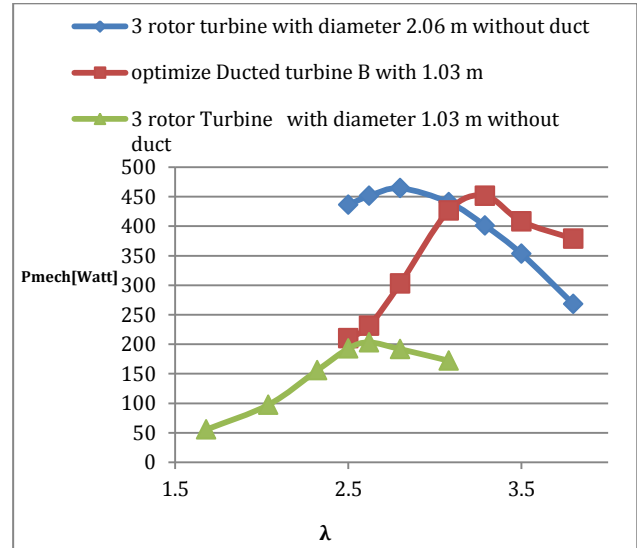


Fig.18 the mechanical power obtained as a function of the tip-speed ratio for $V=9\text{m/s}$

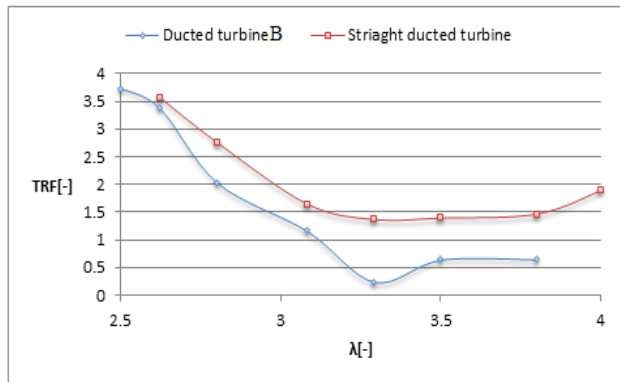


Fig.16 Comparison of torque ripple factor for best straight ducted turbine $\theta_1=85^\circ$ and $\theta_2=45^\circ$ with optimized ducted turbine B, at various TSR

D. Evaluation of Ducted wind turbine regarding space saving

In order to investigate the space saving when using ducted wind turbine compared with naked wind turbine.

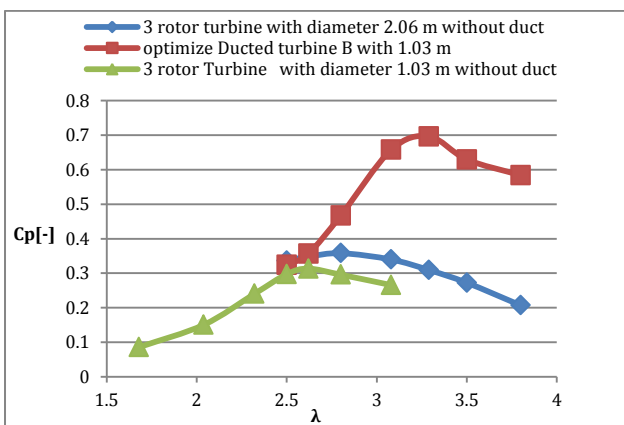


Fig.17 the power coefficient of as a function of the tip-speed ratio for $V=9\text{m/s}$

Estimating of mechanical power for turbine with twice diameter equal 2.06 m compared with optimized ducted turbine B and verified turbine was done. From Fig.17 and Fig.18, it was found that, maximum mechanical power generated in case of ducted turbine B and twice diameter turbine were very close in these values and equal to 451 and 464 watt respectively shows the effect of using duct to save space and increase output mechanical power.

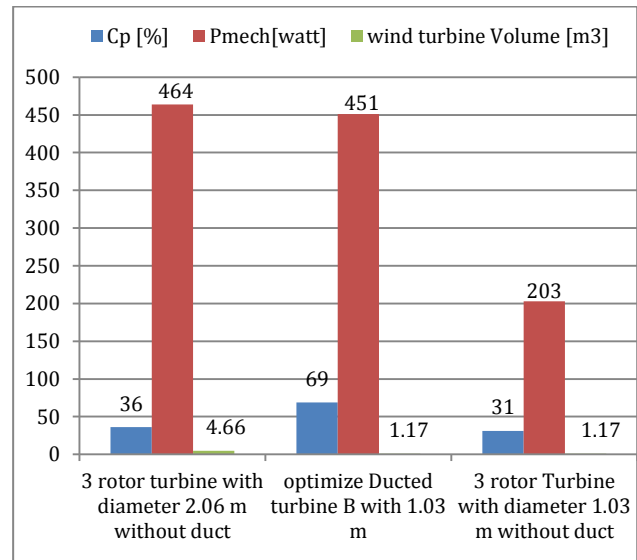


Fig.19 Comparison between ducted turbine and turbine without duct with different diameter

Conclusions

A duct for Darrieus turbine has been designed and its effect on the output of the turbine has been simulated. The results reveal that it is possible to improve the performance of Darrieus turbine on multiple fronts

using an appropriately optimized duct. An attempt was made at optimizing the shape of the duct by studying the effect of the position of the turbine, the convergence angle of the duct and the external shape of the duct on the output of the Darrieus turbine. It was observed that these parameters have an optimum value. The main conclusions from this study are listed below:-

- The turbine position inside duct affects the power coefficient. The best position will be at duct throat, where power performance increased by 120% from turbine without duct.
- Torque ripple was decrease by 84% when the turbine center at the duct throat w.r.t turbine without duct.
- Locating the wind turbine inside a duct decrease the wind turbine volume to 75%, for the same mechanical power.

References

- Berg, D., P. Klimas and W. Stephenson (1990). Aerodynamic design and initial performance measurements for the Sandia 34-m diameter vertical-axis wind turbine. *Ninth ASME Wind Energy Symposium, SED*.
- Castelli, M. R., G. Ardizzon, L. Battisti, E. Benini and G. Pavesi (2010). Modeling strategy and numerical validation for a Darrieus vertical axis micro-wind turbine. *ASME 2010 International Mechanical Engineering Congress and Exposition, American Society of Mechanical Engineers*.
- German, J. (1997). The end of an era: Sandia's 17-meter Vertical Axis Wind Turbine comes down after two decades, *Sandia Lab News* 1997, LN11-21-97.
- Kishore, R. A., T. Coudron and S. Priya (2013). Small-scale wind energy portable turbine (SWEPT). *Journal of Wind Engineering and Industrial Aerodynamics* 116: 21-31.
- Li, S. and Y. Li (2010). Numerical study on the performance effect of solidity on the straight-bladed vertical axis wind turbine. *Power and Energy Engineering Conference (APPEEC), 2010 Asia-Pacific, IEEE*.
- Malipeddi, A. and D. Chatterjee (2012). Influence of duct geometry on the performance of Darrieus hydroturbine. *Renewable Energy* 43: 292-300.
- Mohamed, M. H. A. (2011). Design optimization of savonius and wells turbines. *Ottovon-Guericke University Magdeburg*.
- Mosavi, A. (2010). Multiobjective Optimization of Spline Curves Using Mode Frontier. *Proceedings of International modeFRONTIER Users' Meeting*.
- Musgrove, P. (1987). Wind energy conversion: recent progress and future prospects. *Solar & wind technology* 4(1): 37-49.
- Paraschivoiu, I. (2002). Wind turbine design: with emphasis on Darrieus concept, *Presses inter Polytechnique*.
- Price, T. J. (2006). UK large-scale wind power programme from 1970 to 1990: the Carmarthen Bay experiments and the musgrove vertical-axis turbines. *Wind Engineering* 30(3): 225-242.
- Sivanandam, S. and S. Deepa (2008). Genetic Algorithm Optimization Problems, *Springer*.
- Taher G. Abu-El-Yazied, H. N. D., Ahmad M. Ali and Islam M. Hassan (2014). Investigation of the Aerodynamic Performance of Darrieus Vertical Axis Wind Turbine. *IOSR Journal of Engineering (IOSRJEN)* 04(05): 18-29.